

## Ferroelectric Polarization Flop in a Frustrated Magnet $\text{MnWO}_4$ Induced by a Magnetic Field

K. Taniguchi,<sup>1</sup> N. Abe,<sup>2</sup> T. Takenobu,<sup>3</sup> Y. Iwasa,<sup>3</sup> and T. Arima<sup>1</sup>

<sup>1</sup>*Institute of Multidisciplinary Research for Advanced Materials, Tohoku University, Sendai 980-8577, Japan*

<sup>2</sup>*Department of Physics, Tohoku University, Sendai 980-8578, Japan*

<sup>3</sup>*Institute for Materials Research, Tohoku University, Sendai 980-8577, Japan*

(Received 25 May 2006; published 30 August 2006)

The relationship between magnetic order and ferroelectric properties has been investigated for  $\text{MnWO}_4$  with a long-wavelength magnetic structure. Spontaneous electric polarization is observed in an elliptical spiral spin phase. The magnetic-field dependence of electric polarization indicates that the noncollinear spin configuration plays a key role for the appearance of the ferroelectric phase. An electric polarization flop from the  $b$  direction to the  $a$  direction has been observed when a magnetic field above 10 T is applied along the  $b$  axis. This result demonstrates that an electric polarization flop can be induced by a magnetic field in a simple system without rare-earth  $4f$  moments.

DOI: [10.1103/PhysRevLett.97.097203](https://doi.org/10.1103/PhysRevLett.97.097203)

PACS numbers: 75.80.+q, 64.70.Rh, 77.80.Fm, 77.84.Bw

In the past several years, the coupling between ferroelectric (FE) and magnetic order in multiferroics, where both orders coexist, has been attracting much attention [1]. In particular, a new type of multiferroics such as rare-earth perovskite  $\text{RMnO}_3$  ( $R = \text{Gd, Tb, Dy}$ ), in which FE order appears simultaneously at a magnetic transition, has shown a strong interplay between electric polarization and magnetic order [2,3]. Intriguing phenomena have been found in  $\text{RMnO}_3$  ( $R = \text{Tb, Dy}$ ) such as magnetic-field ( $H$ )-induced electric polarization ( $P$ ) flop [2,3]. In recent studies, some other magnetically frustrated systems are also identified to show similar gigantic magnetoelectric (ME) effects [4–8]. It has been pointed out that there is commonly a close correlation between the long-wavelength magnetic structure and FE order. In particular, the multiferroic materials with long-wavelength magnetic structures appear to be characterized by two key features, which are commensurability and spin chirality (noncollinearity). On the one hand, in systems such as  $\text{RMn}_2\text{O}_5$  ( $R = \text{rare earth and Y}$ ), it has been reported that the locking of the modulation wavelength seems to play a key role for the appearance of the FE phase [9–11]. On the other hands, the systems such as rare-earth perovskite  $\text{RMnO}_3$  ( $R = \text{Gd, Tb, Dy}$ ) are regarded as another type of multiferroic materials, in which the important factor to cause FE transition is a noncollinear spin configuration, but not the change of the modulation wavelength. In fact, it has been confirmed by the neutron diffraction experiments in perovskite  $\text{RMnO}_3$  ( $R = \text{Tb, Tb}_{1-x}, \text{Dy}_x$ ), that the inversion symmetry breaking occurs in transverse spiral spin phase without changing the modulation wavelength [12,13].

As for the mechanism of the FE phase transition at zero magnetic field, recent investigations are identifying the dominant parameters. However, the effect of the magnetic field has not been fully understood. While rare-earth perovskite  $\text{RMnO}_3$  ( $R = \text{Gd-Tb}$ ) and  $\text{RMn}_2\text{O}_5$  ( $R = \text{rare earth element}$ ) are investigated intensively as typical multiferroic systems with long-wavelength magnetic structures,

their responses to magnetic fields are very complex because of the existence of the rare-earth  $f$ -electron moments and crystal structural complexity [14]. For the sufficient understanding of  $H$ -induced gigantic ME effects, it is necessary to investigate multiferroic compounds with only one kind of magnetic ions and a simple ion network. However, the  $H$ -induced sudden  $P$  flop was only observed in perovskite  $\text{RMnO}_3$  with large  $4f$  moments so far to our knowledge. Hence, the  $4f$ - $3d$  exchange interaction might be speculated to be one of the key factors for the  $P$  flop. In this Letter, we report that  $\text{MnWO}_4$  is multiferroic material, which shows ferroelectric  $P$  flop by the application of a magnetic field.  $\text{MnWO}_4$  is a system with long-wavelength magnetic structure [15], and contains only one kind of magnetic ions,  $\text{Mn}^{2+}$ . In this material, it has been found that the spiral spin phase (AF2-phase) plays a dominant role for appearance of the FE phase. In addition, we demonstrate that the direction of the FE polarization can be flopped from the  $b$  to the  $a$  axis by the application of a magnetic field. Since  $\text{MnWO}_4$  contains no rare-earth element, the present results indicate that the  $H$ -induced  $P$  flop can take place without help from  $4f$  moments.

$\text{MnWO}_4$  is crystallized in a wolframite structure, which belongs to the monoclinic space group  $P2/c$  with  $\beta \sim 91^\circ$  at room temperature (see Fig. 1). The crystal structure is characterized by alternative stacking of manganese and tungsten layers parallel to the (100) plane [Fig. 1(b)]. As shown in Fig. 1(a),  $\text{Mn}^{2+}$  ions ( $S = 5/2$ ) are surrounded by distorted oxygen octahedra and aligned in zigzag chains along the  $c$  axis. Although this structure may be regarded as a one-dimensional Heisenberg-spin chain, it is known that three-dimensional long-range antiferromagnetic (AFM) order is realized since the influence of the spins, which are further than the nearest neighbor one, cannot be neglected [16]. While other wolframite  $\text{MWO}_4$  ( $M = \text{Fe, Co, Ni}$ ) show only one magnetic transition to the commensurate magnetic (CM) state with a propagation vector  $\mathbf{k} = (1/2, 0, 0)$ ,  $\text{MnWO}_4$  undergoes successive magnetic

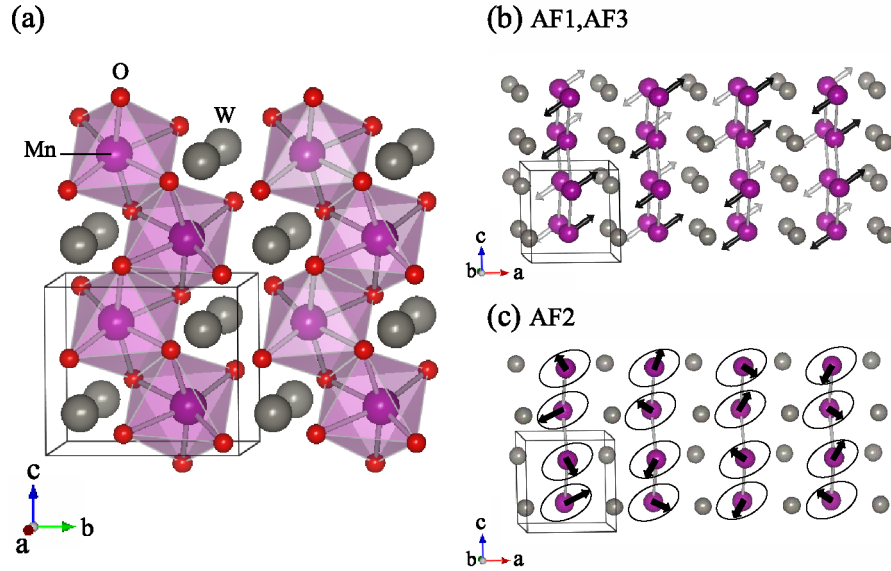


FIG. 1 (color online). (a) Crystal structure of  $\text{MnWO}_4$  viewed along the  $a$  axis: each Mn atom (purple) is surrounded by an oxygen (red) octahedron. W atoms (gray) separate zigzag chains of Mn atoms. (b) Collinear magnetic structure in AF1 and AF3: magnetic moments lie in the  $ac$  plane and canted to the  $a$  axis by about  $35^\circ$ . (c) Elliptical spiral spin structure in AF2: basal plane of spiral is inclined to the  $ab$  plane.

phase transitions at  $\sim 13.5$  K ( $T_N$ ),  $\sim 12.7$  K ( $T_2$ ), and  $\sim 7.6$  K ( $T_1$ ) related to three long-wavelength magnetic ordering states, AF3, AF2, and AF1 [15]. According to the neutron diffraction results, AF1 ( $T < T_1$ ) is a CM-collinear AFM phase, AF2 ( $T_1 < T < T_2$ ) is an incommensurate (ICM) elliptical spiral phase, and AF3 ( $T_2 < T < T_N$ ) is an ICM-collinear AFM phase. The respective propagation vectors are  $\mathbf{k} = (\pm 1/4, 1/2, 1/2)$  for AF1 and  $\mathbf{k} = (-0.214, 1/2, 0.457)$  for AF2 and AF3. In AF1 and AF3, magnetic moments collinearly align in the  $ac$  plane forming an angle of about  $35^\circ$  with the  $a$  axis, whereas in AF2 an additional component in the  $[010]$  direction exists, as shown in Figs. 1(b) and 1(c), respectively [15].

Single crystals of  $\text{MnWO}_4$  were grown by the floating zone method. The resulting crystals appear to be blood red and transparent in thin section. The crystals were oriented using Laue x-ray photographs, and cut into thin plates with wide faces perpendicular to the crystallographic principal axis  $a$  or  $b$ . Gold electrodes were then sputtered onto the opposite faces of the samples for measurements of dielectric constant  $\varepsilon$  and electric polarization  $P$ . We measured  $\varepsilon$  at 1 kHz using a LCR meter, and obtained  $P$  by integration of pyroelectric current, which was measured with an electrometer. The measurements of  $\varepsilon$  and electric polarization  $P$  in a magnetic field up to 14.5 T were performed at the High Field Laboratory for Superconducting Materials, Institute for Materials Research, Tohoku University, Japan. Magnetic susceptibility was measured by a commercial superconducting quantum interference device magnetometer, applying magnetic fields parallel to each crystal principal axis.

Figure 2(a) displays the temperature dependence of the magnetic susceptibility ( $\chi$ ) in a magnetic field of 0.1 T parallel to the  $a$ ,  $b$ , and  $c$  axis, respectively. At Néel temperature,  $T_N \sim 13.5$  K, a cusp is observed in  $\chi$  for all the direction. At higher temperatures than  $T_N$ ,  $\chi(T)$  follows the Curie-Weiss law with a negative Weiss temperature  $\theta$ . We estimated from  $\chi_a$  that  $|\theta|$  is 78 K and the effective moment  $\mu_{\text{eff}}$  is  $6.0 \mu_B$ , which is close to the value  $5.9 \mu_B$  expected from  $\text{Mn}^{2+}$  ( $S = 5/2$ ). It should be noticed here that  $T_N$  is much smaller than  $|\theta|$  in this compound. From the present study, the ratio of  $|\theta|$  to  $T_N$  is estimated to be  $\sim 6$ . This indicates that  $\text{MnWO}_4$  is a spin system with frustration where the antiferromagnetic exchange interactions with the next-nearest neighbor spins should be considered. At the phase transition temperature from AF3 to AF2,  $T_2$ , an appreciable anomaly is observed only in  $\chi_b$ . This would reflect the fact that an additional magnetic component along the  $[010]$  direction arises at  $T_2$  [15]. At  $T_1$ , which is the transition temperature from AF2 to AF1,  $\chi_b$  shows a steep rise, while  $\chi_a$  and  $\chi_c$  show a sharp drop. This behavior is consistent with the neutron diffraction result that the easy axis of the  $\text{Mn}^{2+}$  moments is within the  $ac$  plane in AF1 [15].

Figs. 2(b) and 2(c) show temperature dependence of  $\varepsilon_b$  and  $\Delta P_b$  in zero magnetic field. With decreasing temperature,  $\varepsilon_b$  shows a sharp peak at  $T_2$  and a very small drop ( $\sim 0.08\%$ ), which is displayed in a magnified scale, at  $T_1$ . As seen in Fig. 2(c), the spontaneous polarization exists in the AF2 phase between  $T_1$  and  $T_2$  [17]. We have also confirmed the sign reversal of  $\Delta P_b$  in the AF2 phase with cooling process in a negative electric field (not

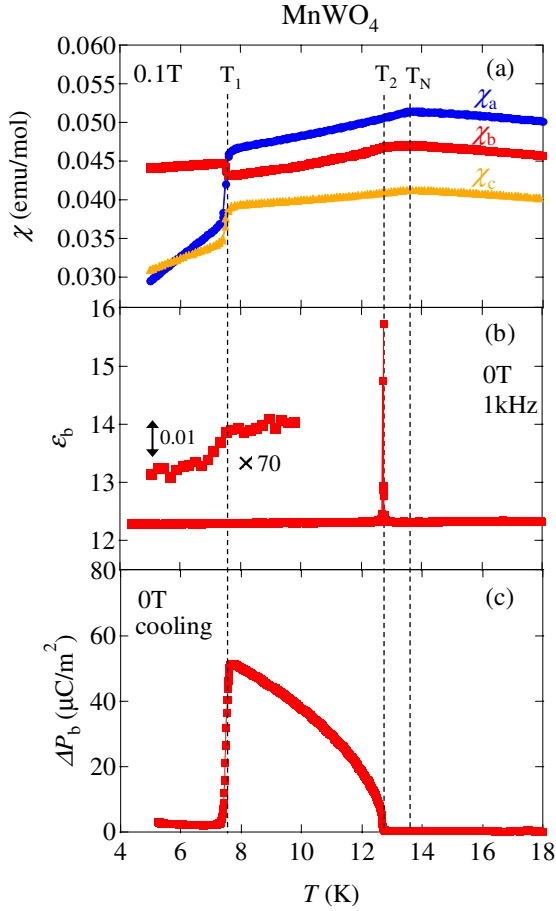


FIG. 2 (color online). (a) Magnetic susceptibility for each crystal axis as a function of temperature in 0.1 T. (b) Dielectric constant for  $E//b$  in 0 T. (c) Electric polarization  $\Delta P//b$  in 0 T. During the measurement of pyroelectric current to obtain  $\Delta P$ , an electric field of 500 kV/m was continuously applied along the  $b$  axis in a cooling process.  $\Delta P$  was calculated by integrating the measured pyroelectric current with respect to time.

shown). These results evidently indicate that  $\text{MnWO}_4$  becomes ferroelectric simultaneously when the AF2 phase with the spiral spin configuration appears. Comparing  $\text{MnWO}_4$  with  $\text{RMnO}_3$  ( $R = \text{Tb, Dy}$ ) [2,3], which also show ferroelectricity in the spiral phase, the maximum of  $P \sim 50 \mu\text{C}/\text{m}^2$  is smaller by more than an order of magnitude. This fact may be related to the difference in orbital momentum  $L$  between  $\text{Mn}^{3+}$  ( $L = 2$ ) and  $\text{Mn}^{2+}$  ( $L = 0$ ). The latter has no net spin-orbit coupling in the ground state.

Figs. 3(a) and 3(b) present the temperature dependence of the electric polarization, which is parallel to the  $b$  and the  $a$  axis, respectively, in several magnetic fields applied parallel to the  $b$  axis. With increasing the magnetic field, the temperature range, where nonzero  $\Delta P_b$ , appears, becomes narrower and  $\Delta P_b$  is suppressed [Fig. 3(a)]. On the other hand, a rapid growth of  $\Delta P_a$  is observed above 10 T [Fig. 3(b)]. In Fig. 3(c) and 3(d), we display the magnetic-

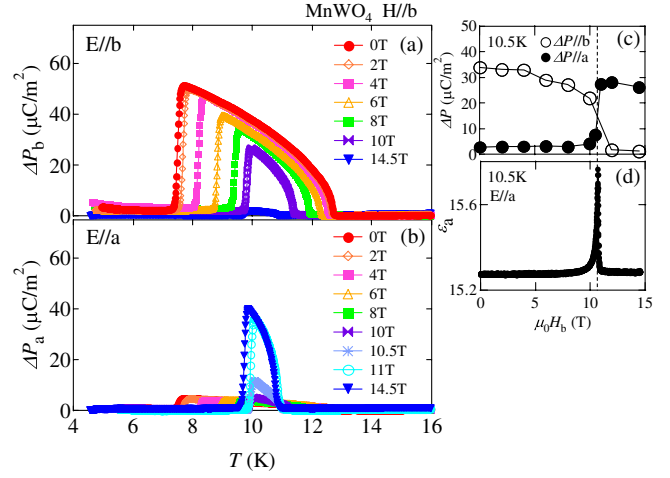


FIG. 3 (color online). (a),(b) Temperature dependence of electric polarization in several magnetic fields. (c) Electric polarization,  $\Delta P$  along the  $b$  (closed circle) and the  $a$  axis (open circle) plotted against the magnetic field at 10.5 K. Plotted values are deduced from (a) and (b). (d) Change in dielectric constant  $\varepsilon//a$  with sweeping the magnetic field at 10.5 K.

field dependence of  $\Delta P$  in each direction and  $\varepsilon_a$  at 10.5 K. Around 10.7 T, where peak anomaly appears in  $\varepsilon_a$ ,  $\Delta P_b$  shows drastic suppression, whereas  $\Delta P_a$  increases sharply. This contrast means that the magnetic field switches the ferroelectric polarization direction from the  $b$  to the  $a$  axis. Although  $\Delta P_a$  shows a small nonzero value in low magnetic fields below 10 T, the observed polarization may be caused by a leak component of  $\Delta P_b$  due to a small misalignment of the sample axis, since the temperature range of  $\Delta P_a$  completely coincides with that of  $\Delta P_b$ .

In Fig. 4, we show the magnetoelectric phase diagram of  $\text{MnWO}_4$  for the direction of magnetic field ( $H$ ) along the  $b$  axis. Closed and open squares represent the data points in the cooling (or  $H$  decreasing) and warming (or  $H$  increasing) runs of pyroelectric current (or  $\varepsilon$ ) measurements, respectively. Reflecting the first-order-like change in  $\chi$  and  $\Delta P$ , hysteresis is observed at  $T_1$ . On the other hand, hysteresis is hardly observed at  $T_2$ . Since  $\chi$  and  $\Delta P$  show continuous change, the phase transition between AF2 and AF3 would be a second-order one. These results are in a good agreement with the fact that the jump of the magnetic propagation vector is only observed at  $T_1$  [15]. According to the previously reported magnetic phase diagram [18], the FE phase with  $P//b$  is identical with the elliptical spiral spin phase, AF2. This fact demonstrates that the noncollinear spin configuration plays a key role in the FE phase of  $\text{MnWO}_4$ .

Several groups have been proposed for the mechanism of magnetically driven ferroelectricity for noncollinear magnets [6,19,20]. The microscopic model taking into account the spin-orbit interaction [19] predicts that the  $P$  direction should be given by  $\langle e_{ij} \times (\mathbf{S}_i \times \mathbf{S}_j) \rangle$ , in which  $e_{ij}$  is the unit vector connecting two magnetic ions and  $\mathbf{S}_a$

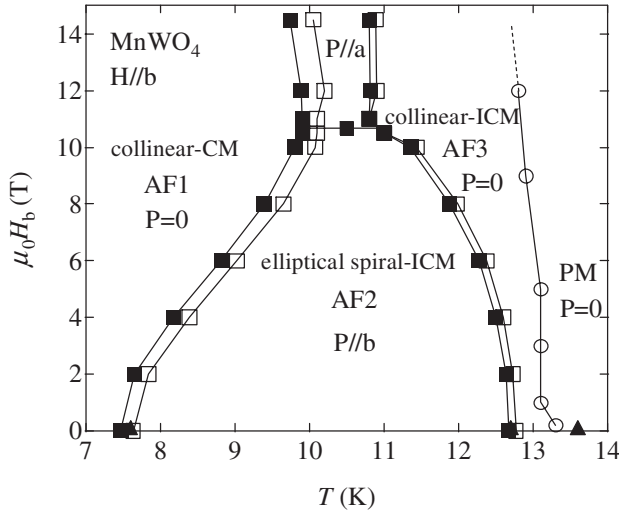


FIG. 4. Magnetoelectric phase diagram of  $\text{MnWO}_4$  in magnetic fields parallel to the  $b$  axis. Closed and open squares represent the data points in the cooling (or  $H$  decreasing) and warming (or  $H$  increasing) runs of pyroelectric current (or  $\epsilon$ ) measurements, respectively. Closed triangles show magnetic phase transition temperatures determined by the magnetic susceptibility measurements in a cooling run in the present study. Open circles represent the Néel temperatures reported by another group [18].

( $\alpha = i, j$ ) is a magnetic moment at the  $\alpha$  site. Since the basal plane of the spiral is reported to be inclined to the  $ab$  plane about  $34^\circ$  [15], the  $\mathbf{S}_i \times \mathbf{S}_j$  lies in the  $ac$  plane forming an angle of about  $124^\circ$  with the  $a$  axis. Taking into account that the  $\text{Mn}^{2+}$  chain is along the  $c$  axis ( $\langle e_{ij} \rangle = [001]$ ), the predicted  $P$  direction is along the  $b$  axis, which is in a good agreement with the present results (See Fig. 3).

As displayed in Fig. 4, the new FE phase with  $P$  parallel to the  $a$  axis has also been found in magnetic fields higher than 10 T. Since a jump of magnetization has been reported around the phase boundary in the previous research [18], the  $P$  flop would be caused by a phase transition to a new magnetic phase, which is different from AF1, AF2, and AF3. The identification of this new magnetic phase is a future issue.

In summary, we have identified  $\text{MnWO}_4$  as a multi-ferroic compound in which magnetic and ferroelectric orders coexist in the same temperature range. The magnetic-field dependence shows the close relation between the stability of ICM-elliptical spiral AF2 and the appearance of spontaneous polarization parallel to the  $b$  axis. This fact means that the noncollinear spin configuration plays a key role for the ferroelectricity in  $\text{MnWO}_4$ . It is also found that the electric polarization flops from the  $b$  to the  $a$  axis when the magnetic field is applied along the  $b$  axis. This is the first example of the ferroelectric polar-

ization flop induced by magnetic fields in transition-metal oxide systems without rare-earth  $4f$  moments.

We thank M. Saito and S. Otani for help with experiments. This work was partly supported by Grants-In-Aid for Scientific Research from the MEXT Japan.

- [1] M. Fiebig, *J. Phys. D* **38**, R123 (2005).
- [2] T. Kimura, T. Goto, H. Shintani, K. Ishizaka, T. Arima, and Y. Tokura, *Nature (London)* **426**, 55 (2003).
- [3] T. Goto, T. Kimura, G. Lawes, A.P. Ramirez, and Y. Tokura, *Phys. Rev. Lett.* **92**, 257201 (2004).
- [4] N. Hur, S. Park, P.A. Sharma, J.S. Ahn, S. Guha, and S.-W. Cheong, *Nature (London)* **429**, 392 (2004).
- [5] T. Kimura, G. Lawes, and A.P. Ramirez, *Phys. Rev. Lett.* **94**, 137201 (2005).
- [6] G. Lawes, A. B. Harris, T. Kimura, N. Rogado, R. J. Cava, A. Aharony, O. Entin-Wohlman, T. Yildirim, M. Kenzelmann, C. Broholm, and A. P. Ramirez, *Phys. Rev. Lett.* **95**, 087205 (2005).
- [7] T. Kimura, J. C. Lashley, and A. P. Ramirez, *Phys. Rev. B* **73**, 220401(R) (2006).
- [8] Y. Yamasaki, S. Miyasaka, Y. Kaneko, J.-P. He, T. Arima, and Y. Tokura, *Phys. Rev. Lett.* **96**, 207204 (2006).
- [9] L. C. Chapon, G. R. Blake, M. J. Gutmann, S. Park, N. Hur, P. G. Radaelli, and S.-W. Cheong, *Phys. Rev. Lett.* **93**, 177402 (2004).
- [10] L. C. Chapon, P. G. Radaelli, G. R. Blake, S. Park, and S.-W. Cheong, *Phys. Rev. Lett.* **96**, 097601 (2006).
- [11] H. Kimura, Y. Kamada, Y. Noda, K. Kaneko, N. Metoki, and K. Kohn, *cond-mat/0602226*.
- [12] M. Kenzelmann, A. B. Harris, S. Jonas, C. Broholm, J. Schefer, S. B. Kim, C. L. Zhang, S.-W. Cheong, O. P. Vajk, and J. W. Lynn, *Phys. Rev. Lett.* **95**, 087206 (2005).
- [13] T. Arima, A. Tokunaga, T. Goto, H. Kimura, Y. Noda, and Y. Tokura, *Phys. Rev. Lett.* **96**, 097202 (2006).
- [14] T. Goto, Y. Yamasaki, H. Watanabe, T. Kimura, and Y. Tokura, *Phys. Rev. B* **72**, 220403(R) (2005).
- [15] G. Lautenschläger, H. Weitzel, T. Vogt, R. Hock, A. Böhm, M. Bonnet, and H. Fuess, *Phys. Rev. B* **48**, 6087 (1993).
- [16] H. Ehrenberg, H. Weitzel, H. Fuess, and B. Hennion, *J. Phys. Condens. Matter* **11**, 2649 (1999).
- [17] Although there is a small nonzero polarization in the AF1 phase, it is within experimental error, which arises from the background noise ( $\sim 0.5$  pA) in the pyroelectric current integrating process. Concerning the effect of nonzero electric field effect on the observed  $P$  value, we confirmed that the AF2 phase shows almost the same magnitude of  $P$  in field-cooled–zero-field-warming runs as in a field cooling run. Therefore, the influence of an applied electric field for  $P$  values seems to be small enough.
- [18] H. Ehrenberg, H. Weitzel, C. Heid, H. Fuess, G. Wltschek, T. Kroener, J. van Tol, and M. Bonnet, *J. Phys. Condens. Matter* **9**, 3189 (1997).
- [19] H. Katsura, N. Nagaosa, and A. V. Balatsky, *Phys. Rev. Lett.* **95**, 057205 (2005).
- [20] M. Mostovoy, *Phys. Rev. Lett.* **96**, 067601 (2006).